Anomalous magnetoresistance of nonequilibrium Eu-TM (Co, Mo) alloy thin films

1998 J. Phys.: Condens. Matter 10 5619

(http://iopscience.iop.org/0953-8984/10/25/012)

J. Phys.: Condens. Matter **10** (1998) 5619–5626. Printed in the UK PII: S0953-8984(98)89897-4

Anomalous magnetoresistance of nonequilibrium Eu–TM (Co, Mo) alloy thin films

T J Konno, K Wakoh, K Shoji, K Sumiyama and K Suzuki
Institute for Materials Research, Tohoku University, Sendai 980-8577, Japan

Received 8 December 1997

Abstract. We studied the magnetization and magnetoresistance ratio (MR) of nonequilibrium Eu-rich Eu–TM (TM = Co, Mo) alloy thin films prepared by vapour-phase synthesis. We observed that the magnetization curves of the Eu–TM films show an irreversible kink at about 8 T. The longitudinal and transverse MR curves of these films also exhibit irreversible positive-to-negative change at about 8 and 4 T, respectively, while reversible components show only a monotonic decrease. These behaviours are in contrast with the monotonically increasing MR of pure Eu, measured up to 14 T, but are essentially identical to those observed for nonequilibrium Eu–Fe thin films, implying that the anomaly results from structural disorder rather than from the magnetic moments of impurities.

1. Introduction

The magnetic moments of the bcc-Eu metal order helically below the Néel temperature, 90 K [1, 2]. Magnetization increases gradually with the lifting of the moments out of the helical plane into the field direction [3–5], while the corresponding magnetoresistance ratio (MR), measured up to 8 T, increases monotonically [6]. Nonequilibrium Eu–Fe thin films prepared by co-evaporation show quite different behaviours: the magnetization curve, measured up to 23 T, shows an irreversible kink at about 8 T, while longitudinal MR (L-MR) and transverse MR (T-MR) undergo an anomalous change from positive to negative values at about 8 and 4 T, respectively [7]. These observations indicate that the introduction of Fe into the Eu metal modifies the magnetic character of Eu. However, it is not clear whether or not the above anomalous behaviours arise from the magnetic moments of dissolved Fe or from a structural disorder alone. Therefore, we prepared nonequilibrium Eu-rich Eu–Co and Eu–Mo thin films, and studied their magnetic and transport behaviours.

In order to distinguish between the effect of magnetic moments and structural disorder, we chose Co and Mo since the former is a ferromagnetic transition metal, like Fe, and the latter does not possess a magnetic moment. We know from the equilibrium phase diagram of the Eu–Mo system that Eu and Mo are immiscible with each other, but the existence of a similar diagram for the Eu–Co system has yet to be confirmed [8]. This suggests that the vapour-phase synthesis of Eu-rich Eu–Co and Eu–Mo films will likely result in a bcc-Eu phase supersaturated with Co and Mo, respectively. Given the lack of data on the MR of pure Eu above 8 T, we also measured the MR of a pure Eu thin film in fields up to14 T. Our results show that the Eu–Mo system, like the Eu–Co system, exhibits similar types of anomalous behaviour as those summarized above for the Eu–Fe system, implying that the anomaly arises from a structural disorder alone.

0953-8984/98/255619+08$19.50

2. Experimental procedures

Eu–Co nonequilibrium thin films of about 1 μm in thickness were prepared by co-evaporation. For the Co source, we used zirconia and molybdenum for the inner and outer crucibles, respectively, and a molybdenum crucible for the Eu source. These crucibles were placed about 0.2 m away from the substrate position in a vacuum chamber. The base pressure of the chamber, obtained with a diffusion pump, was about 10^{-4} Pa. A few grams of Co metal were heated by electron bombardment, while roughly the same amount of Eu metal was heated by conventional radiation with tungsten filaments. The purity of both metals was 99.99%. The deposition rates of Eu and Co were monitored using an oscillation thickness sensor. To prepare Eu–Mo films, we installed an ion-beam sputtering gun inside the deposition chamber described above [9, 10]. Thus, Mo was sputter deposited, while Eu was evaporated, resulting in the formation of a nonequilibrium Eu–Mo thin film. We used polyimide films and Si wafers as substrate for magnetic and structural characterization. The deposition was carried out at room temperature. Our preliminary work showed that temperature rise is negligible during deposition.

We used a Rigaku x-ray diffractometer equipped with a Cu target, in the standard Bragg–Brentano geometry, for the x-ray diffraction (XRD) study. The chemical composition of deposited films was determined by electron probe microanalyser (EPMA). For Eu–Mo films, the composition was cross-examined by inductively coupled plasma mass spectroscopy (ICP-MS), which confirmed that the possibility of Fe contamination in the films is negligible. The magnetic moments of the films up to 23 T at 4.2 K were measured employing an extraction method in a hybrid-type high-field magnet [11]. In this report, we expressed observed magnetic moments in terms of Bohr magnetons, μ_B, per atom, averaged over Eu and TM (Co or Mo) according to composition. A standard DC four-probe method was used to measure the electrical resistivities of specimens at 4.2 K in magnetic fields up to 14 T applied parallel or perpendicular to the current direction. We repeated the MR measurements twice so as to observe any possible hysteretic behaviour. T-MR was measured immediately after each L-MR measurement, using the same specimen. MR is defined by $\Delta\rho(H)/\rho(0) = [\rho(H) - \rho(0)]/\rho(0)$, where $\rho(H)$ is electrical resistivity as a function of magnetic field, H.

3. Results

The XRD patterns of $Eu_{62}Co_{38}$ and $Eu_{85}Mo_{15}$ films shown in figure 1 indicate that peaks due to the bcc-Eu phase are by far the strongest, suggesting that the films are comprised predominantly of the bcc-Eu phase. The presence of small peaks due to EuO indicates that a part of Eu was oxidized. However, no peaks due to Co or Mo were observed; the $\{10\cdot0\}$, $\{00\cdot2\}$, and $\{10\cdot1\}$ peak positions of hcp-Co were 42°, 45° and 47°, respectively, while the {110} and {200} peak positions of bcc-Mo were 41° and 59°, respectively. The XRD patterns of other compositions made in this study did not show any peaks due to Co or Mo phases either. Thus, it may be said that Co and Mo are dissolved or supersaturated in a bcc-Eu matrix.

Figure 2 shows the magnetization curves of $Eu_{84}Co_{16}$ and $Eu_{90}Mo_{10}$ films. Both curves exhibit an initial rise to about 1 μ_B/atom within 1 T, followed by a gradual increase. The slope of the curve increases in the 5–8 T range, resulting in a small, but definite 'kink'. Afterwards, magnetization increases monotonically, but does not saturate even at 23 T. With decreasing field, magnetization decreases monotonically, without revealing any kink.

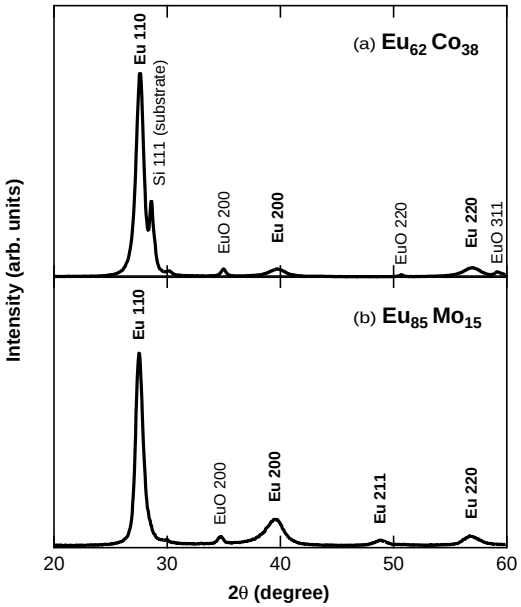

Figure 1. XRD patterns of (a) $Eu_{62}Co_{38}$ and (b) $Eu_{85}Mo_{15}$ films, showing that the films consist mainly of the bcc-Eu phase. No peaks due to hcp-Co or bcc-Mo were found.

Thus, the curve with decreasing field deviates from that with increasing field below 8 T, and results in residual magnetization, as shown in the insets.

Table 1 compares the zero field resistivities of the pure Eu, $Eu_{89}Co_{11}$ and $Eu_{90}Mo_{10}$ films at 293 K, ρ_{293}, with those at 4.2 K, $\rho_{4.2}$. As shown, Eu–TM films have larger resistivity values than pure Eu, but smaller resistivity ratios ($\rho_{293}/\rho_{4.2}$). These observations underscore the role of impurity scattering in the transport behaviour of alloy films. However, the $\rho_{293}/\rho_{4.2}$ value of 11 observed for the pure Eu film is still smaller than the reported $\rho_{300}/\rho_{4.2}$ value of about 150 for an annealed bulk specimen [12]. This discrepancy indicates that the pure Eu film prepared here still contains a large amount of structural defects.

Table 1. Resistivity of pure Eu, $Eu_{89}Co_{11}$ and $Eu_{90}Mo_{10}$ films at 293 K, ρ_{293}, and at 4.2 K, $\rho_{4.2}$. The ratios of ρ_{293} to $\rho_{4.2}$ for the films are also shown.

	ρ_{293} ($\mu\Omega$ m)	$\rho_{4.2}$ ($\mu\Omega$ m)	$\rho_{293}/\rho_{4.2}$
Pure Eu film	0.83	0.074	11
$Eu_{89}Co_{11}$ film	1.78	0.59	3.0
$Eu_{90}Mo_{10}$ film	1.30	0.79	1.2

Figure 3 shows the MR of $Eu_{95}Co_5$ and $Eu_{89}Co_{11}$ films. We observe an increase to 0.05 in the L-MR of the $Eu_{95}Co_5$ film at about 7 T, followed by a decrease to 0.02 at about 10 T, and ultimately a slightly increasing curve. With decreasing field, the L-MR deviates considerably from the initial curve below 7 T, resulting in a residual value of approximately 0.07. The L-MR of the second run is practically identical to that of the second half (decreasing field) of the first run. On the other hand, the T-MR shows only

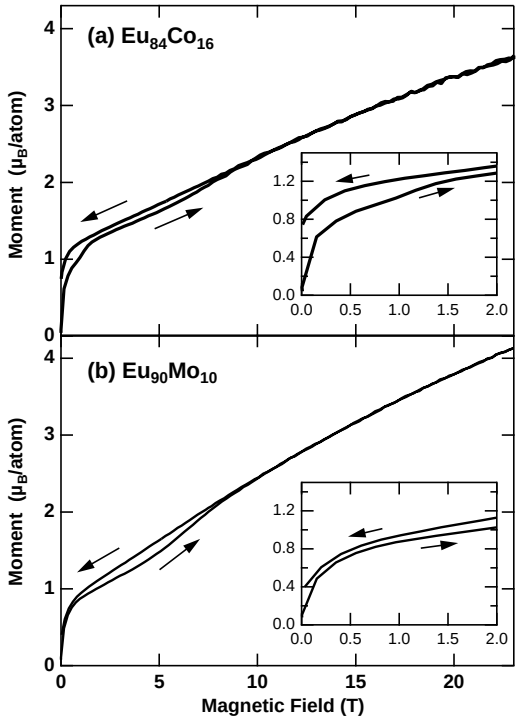

Figure 2. Magnetization curves of (a) $Eu_{84}Co_{16}$ and (b) $Eu_{90}Mo_{10}$ films. The arrows indicate increasing and decreasing fields. Both samples exhibit an irreversible kink at around 8 T. Residual magnetizations are indicated in the insets.

a small increase to about 0.01 at about 4 T, followed by a rapid decrease, resulting in a negative MR of about -0.08 at about 10 T, and again a slight increase up to 14 T. With decreasing field, the T-MR shows an overall increase, resulting in a residual value of -0.05. In the second run, the T-MR deviates towards positive values from the decreasing half of the first run, until it merges into the first curve at about 10 T. The T-MR with decreasing field, on the other hand, is the same as that of the first run. The L- and T-MR of the $Eu_{89}Co_{11}$ thin film (figure 3(b)) can be considered to possess basically the same features as those of the $Eu_{95}Co_5$ film, except that, here, the curves exhibit a monotonic decrease above 10 T. Also, as the Co content of films increases, the deviation of T-MR in the second run from that of the first run diminishes. The MRs of Eu–Co films with other compositions exhibit similar behaviours.

Figure 4 shows the MR of $Eu_{90}Mo_{10}$ and $Eu_{85}Mo_{15}$ films. The curves possess essentially the same features as those of the Eu–Co thin films: the L-MR and T-MR of Eu–Mo films can be separated into reversible and irreversible components. The reversible components show a monotonically decreasing curve. The irreversible component of L-MR is positive, while that of the T-MR is negative. These observations are also in agreement with those made on the Eu–Fe films [7].

Figure 5 shows the MR of the pure Eu thin film. Both L- and T-MR exhibit a monotonic increase up to 14 T. The relatively wide scattering of the data is the result of the low $\rho(0)$

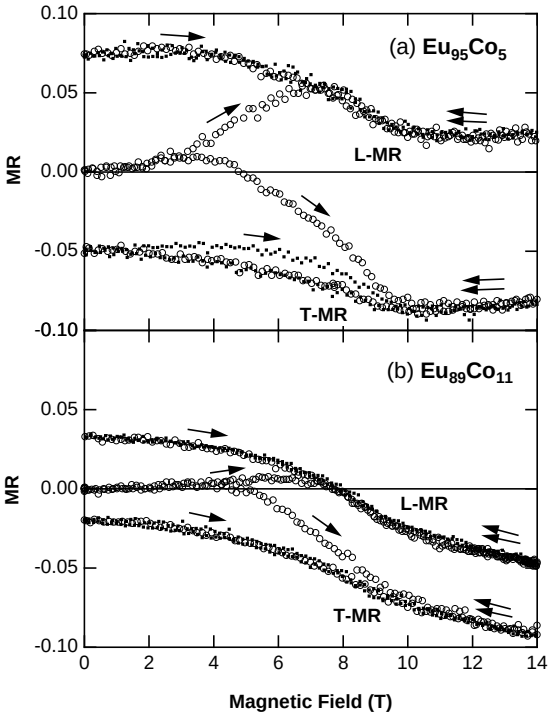

Figure 3. L- and T-MR of (a) $Eu_{95}Co_5$ and (b) $Eu_{89}Co_{11}$ films. Open circle: first run; dots: second run. In the first run, L-MR and T-MR exhibit large hystereses, resulting in positive and negative MR values, respectively. The second run yields reversible, decreasing MR curves, though the T-MR of the $Eu_{95}Co_5$ film shows a small hysteresis.

value of about 0.07 $\mu\Omega$ m (table 1), which is one order lower than the values of Eu–TM alloy films. We fitted the MR data by a simple polynomial function (shown in the figure to guide the eyes) together with error bars corresponding to the standard deviations of the data from each fitted curve. The resulting L-MR values were about 0.3 and 0.5 at 8 and 14 T, respectively. These values are very similar to the approximate value of 0.45 at 8 T that was obtained for a bulk specimen by Jánôs *et al* [6]. Considering that thin films, as opposed to bulk materials, normally contain various structural defects, we can suppose that the discrepancies in the L-MR values arise mainly from different $\rho(0)$ values. Jánôs *et al* also reported that L-MR exhibits a tendency to saturate at around 8 T. However, figure 5 shows that only a slight decrease in the slope appears at around 6 T, and that the L-MR increases monotonically up to 14 T. On the other hand, the residual L-MR value of about 0.1 that we obtained is in good agreement with the data presented by them. The T-MR also increases monotonically with an increase in the slope at about 6–7 T. As far as we know, the T-MR of pure bulk Eu has been reported only up to 2 T at 20.4 K by Boyarskii and Dikovskii [12]. Their data reveal an initial decrease, followed by a monotonic increase with a negative residual T-MR of -0.06. The T-MR of the Eu thin film, which was obtained at 4.2 K (figure 5), does not exhibit a similar initial decrease, but there is indeed a negative residual T-MR of about -0.1.

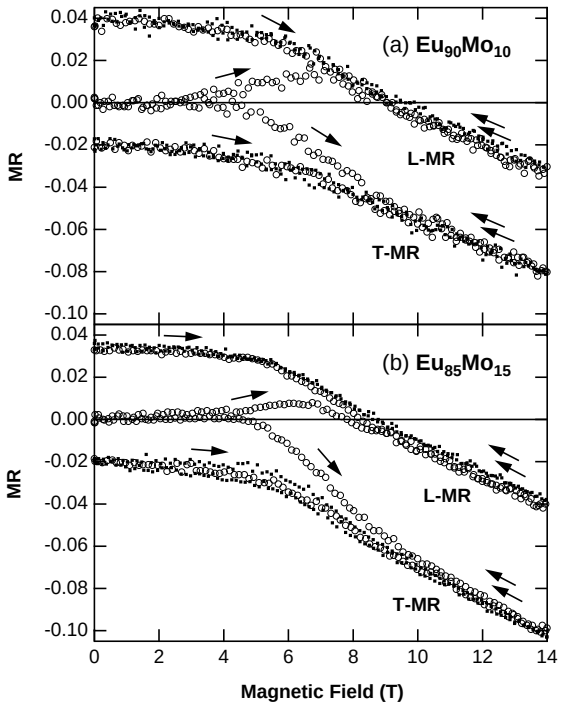

Figure 4. L- and T-MR of (a) $Eu_{90}Mo_{10}$ and (b) $Eu_{85}Mo_{15}$ films. Open circle: first run; dots: second run. These curves are characterized by irreversible and reversible components, the same features that were observed in the Eu–Co films.

4. Discussion

In the present study, we showed that the L- and T-MR of a pure Eu thin film exhibit only a positive monotonic increase up to 14 T, and that the anomalies observed in the Eu–TM thin films result from alloying. Importantly, we found anomalies in the Eu–Mo films, and thus argued that these phenomena do not originate from magnetic moments of TM elements, but strictly from a structural disorder. In this section, we will first briefly compare the MR behaviour of a pure Eu film with that of bulk material, and then discuss the anomalous MR behaviours of Eu–TM films.

Boyarskii and Dikovskii separated the irreversible from the reversible MR components of annealed bulk Eu metal [12]. Based on their findings, they claimed that the irreversible component is due to the reorientation of the helix axes, rather than to a simple domain wall scattering. They also sustained that the critical field at which the irreversible component vanishes is below 0.8 T. The MR data obtained in this study for a pure Eu film (figure 5) show that the critical field is slightly above this value. This discrepancy may be the result of a difference in specimen quality, i.e., annealed bulk material versus vapour-synthesized film, the latter containing large amounts of defects, as can be inferred from the different $\rho_{293}/\rho_{4.2}$ values discussed above.

The anomalous transport behaviours of the Eu–TM films are characterized by a positive-to-negative transition of the irreversible part of the MR curves. This behaviour was also observed in the Eu–Fe films [7]. As mentioned earlier, Eu metal possesses a helical spin

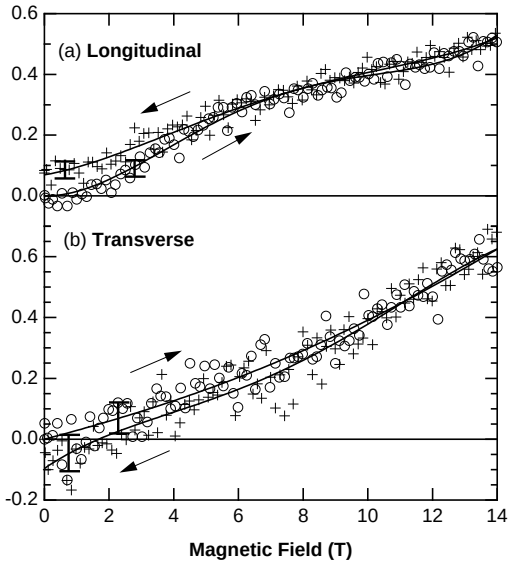

Figure 5. L- and T-MR of a pure Eu film. Open circles: increasing field; crosses: decreasing field. The fitted curves serve to guide the eyes (see text). Both curves exhibit monotonically increasing MR. Small positive and negative residual MRs can be seen for L- and T-MR, respectively.

structure, and magnetization proceeds via lifting of helically ordered moments toward a field direction, forming a conical spin structure [1–3]. On the other hand, calculations by Yamada and Takada indicate that the MR of a simple, two-sublattice antiferromagnet initially increases, since spin fluctuation in the sublattice anti-parallel to the applied field also increases with the applied field [13, 14]. Therefore, in order to explain the anomalous MR behaviours of Eu–Fe and Eu–TM films, we can postulate that, due to the presence of impurities, a small number of Eu spins are initially found outside the helical plane, and that under an external field, enhanced fluctuation of the metastable spins with components anti-parallel to the field direction give rise to a positive MR. This effect prevails until the spin-flop transition occurs, after which the MR decreases. The kink in the magnetization curves also arises from spin-flop transition at the critical field. Thus, the spin fluctuation model seems to explain the observed anomalous MR and magnetization behaviours reasonably well.

In addition, it should be noted that the tilting of the helix axis within a small cone gives rise to the same configuration as that observed when the random scatterings of the spins outside of the helical plane are small. That is, the random scattering of the spins and the tilting of the helix axis are two equivalent views for the same phenomenon. By neutron diffraction on single-crystal Eu, Millhouse and McEwen showed that the critical field necessary to stabilize the helix axis primarily depends on the initial orientation of the crystal: a field of 0.7 T is sufficient for domains having the helix axis perpendicular to the applied field, but a much higher field is needed for domains having the helix axis at 45° from the applied field [3]. These observations suggest that the reorientation of the helix axis is rather sensitive to the environment, and depends on a number of factors, such as the orientation of the crystal, the presence of defects etc. In other words, it can be suggested that structural defects caused by impurities, such as Fe, Co or Mo, can effectively act to retard the reorientation process. In addition, the magnetization data (figure 2) allow us to

suggest that the spin-flop or reorientation of the helix axis takes place rather gradually and concludes at an external field strength of approximately 8 T, although further theoretical study is needed to quantitatively explain the observed critical field strength.

5. Conclusions

We prepared nonequilibrium Eu-rich Eu–Co and Eu–Mo thin films by vapour-phase syntheses. The XRD patterns of the films did not show any peaks due to the transition-metal phase, implying that Co or Mo is supersaturated in the bcc-Eu phase. The magnetization curves of the above alloy films exhibited an irreversible kink at about 8 T, while their L- and T-MR changed irreversibly at 8 and 4 T, respectively. The irreversible components of L- and T-MR were positive and negative, respectively, while the reversible components showed only a decreasing MR. The fact that these anomalies are found both in the Eu–Co and Eu–Mo alloy systems suggests that they are due to structural defects alone, and not to the magnetic moments of impurities.

Acknowledgments

The authors thank Dr S Mitsudo and Mr Y Nakanishi for the magnetization measurements performed in the High Field Laboratory for Superconducting Materials, Tohoku University. They also appreciate Mr Y Murakami for the EPMA analysis, in the Laboratory for Developmental Research of Advanced Materials, IMR, Tohoku University. This work was supported by grants-in-aid for scientific research (A-2: 08405043 and C:08875127) and for scientific research on priority areas (06244106), provided by the Ministry of Education, Science, Sports and Culture of Japan.

References

[1] Olsen C E, Nereson N G and Arnold G P 1962 *J. Appl. Phys.* **33** 1135
[2] Nereson N G, Olsen C E and Arnold G P 1964 *Phys. Rev.* **135** 176
[3] Millhouse A H and McEwen K A 1973 *Solid State Commun.* **13** 339
[4] Nagamiya T, Nagata K and Kitano Y 1962 *Prog. Theor. Phys.* **27** 1253
[5] McEwen K A 1978 *Handbook on the Physics and Chemistry of Rare Earths* vol 1, ed K A Gschneidner Jr and L Eyring (Amsterdam: North-Holland) p 411
[6] Jánôs S, Feher A and Flachbart K 1977 *Phys. Status Solidi* b **81** K19
[7] Konno T J, Ogawa N, Wakoh K, Sumiyama K, Shoji K, Onodera H, Suzuki K and Katoh H 1998 *J. Phys.: Condens. Matter* **10** 5627
[8] Massalski T B 1990 *Binary Alloy Phase Diagrams* 2nd edn, vol 2, ed T B Massalski (Materials Park, OH: ASM) p 1659
[9] Kaufman H R, Cuomo J J and Harper J M E 1982 *J. Vac. Sci. Technol.* **21** 725
[10] Harper J M E, Cuomo J J and Kaufman H R 1982 *J. Vac. Sci. Technol.* **21** 737
[11] Nakagawa Y, Noto K, Hoshi A, Miura S, Watanabe K and Muto Y 1984 *J. Physique* **45** 771
[12] Boyarskii L A and Dikovskii V Y 1976 *Sov. J. Low Temp. Phys.* **2** 632
[13] Yamada H and Takada S 1973 *J. Phys. Soc. Japan* **34** 51
[14] Yamada H and Takada S 1973 *Prog. Theor. Phys.* **49** 1401